Hindawi Publishing Corporation
Journal of Nanomaterials
Volume 2015, Article ID 451834, 7 pages
http://dx.doi.org/10.1155/2015/451834

Research Article

Parametric Studies on Artificial *Morpho* Butterfly Wing Scales for Optical Device Applications

Hyun Myung Kim,[1] Sang Hyeok Kim,[1] Gil Ju Lee,[1] Kyujung Kim,[2] and Young Min Song[1]

[1]*Department of Electronics Engineering, Pusan National University, Busan 609-735, Republic of Korea*
[2]*Department of Nanofusion Technology, Pusan National University, Miryang 627-706, Republic of Korea*

Correspondence should be addressed to Kyujung Kim; k.kim@pusan.ac.kr and Young Min Song; ysong@pusan.ac.kr

Received 10 August 2015; Revised 5 October 2015; Accepted 7 October 2015

Academic Editor: Abdelwahab Omri

We calculated diffraction efficiencies of grating structures inspired by *Morpho* butterfly wings by using a rigorous coupled-wave analysis method. The geometrical effects, such as grating width, period, thickness, and material index, were investigated in order to obtain better optical performance. Closely packed grating structures with an optimized membrane thickness show vivid reflected colors and provide high sensitivity to surrounding media variations, which is applicable to vapor sensing or healthcare indicators. *Morpho* structures with high index materials such as zinc sulfide or gallium phosphide generate white color caused by broadband reflection that can be used as reflected light sources for display applications.

1. Introduction

Many species of insects display vivid color that is widely known as structural color caused by optical interference [1, 2]. Butterflies are famous for their brilliant iridescent colors, which arise from the photonic-nanostructures on the scales on their wings [3–5]. The multifunctional characteristics of *Morpho* butterfly wing scales, including lightweight, visual effects, hydrophobicity, and mechanically strong and thermal regulations, are revealed and have a relationship with the photonic structures in the ridges of the scales. The optical properties depend strongly on the wavelength, incident angle of light, and viewing angle. Several research groups analysed the structure of the wings of *Morpho* butterflies in order to understand their blue vivid iridescence (Figure 1) [6–8]. It is commonly believed that the multilayer interference from the stack of lamellae of regular periodic ridges on the scale is the origin of the blue iridescence of the *Morpho* butterflies. This is the basic reason of butterfly's sensitivity to environmental surrounding media. The brightness and color can be changed with the alteration of surrounding media. Some researchers suggested that this special property could be implemented into the engineering designs for highly sensitive vapor/gas sensors or healthcare optical indicators [9–15]. Tunable photonic circuits, optical computing, less harmful pigments, and photonic papers were also suggested as potential applications [16].

In recent years, artificial *Morpho* structures were developed by using various nanofabrication techniques such as focused ion beam methods [17], e-beam lithography [11, 18], laser interference lithography [19], and multilayer deposition of two different materials [16, 20, 21]. Since these structures are originated from the natural *Morpho* wings, reported works mainly focus on the mimicking "original" structures with similar refractive index. It is known that the "Christmas tree" like structure with refractive index of ~1.5 provides superior optical performance to that of other simple grating structures [22, 23]. However, it causes complicate fabrication procedures. Hence, it is mandatory to determine an optimum geometry of artificial structures by considering the fabrication tolerances and material issues. In this study, we have calculated the diffraction efficiency of the *Morpho* structures on various materials with different thicknesses (slab and air), widths (lamella and ridge), and periods. Optimum geometries are discussed in terms of reflectance, grating structures, and tuning capabilities.

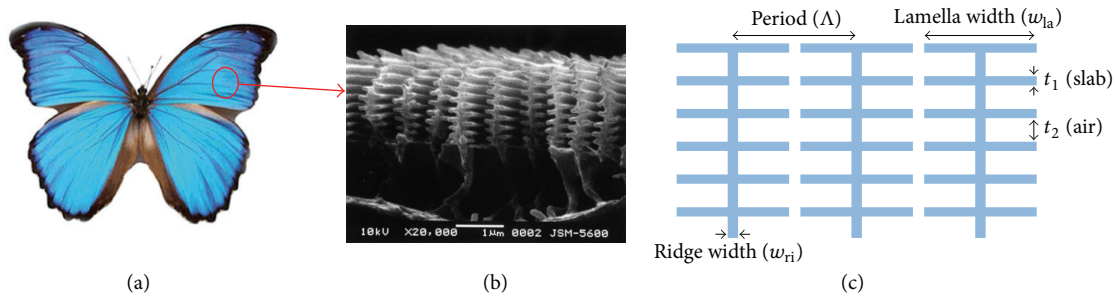

FIGURE 1: (a) Image of a *Morpho* butterfly and (b) cross-sectional SEM image of wing scales (copyright: Kinoshita and Yoshioka [3]) and (c) schematic illustration of *Morpho* photonic structures used in the calculation.

2. Simulation Results and Discussion

Figure 1(c) shows schematic illustrations of simple grating like structures, similar to *Morpho* wing nanostructures, used in this simulation. The initial parameters (i.e., period, width of ridge and lamella, thickness of slab and air gap, and number of slabs) were selected by observing a scanning electron microscope (SEM) image of *Morpho* wing scales (Figure 1(b)). For simplicity, we neglected the tapering or inclining of the ridge structures observed in the SEM image. In this calculation, we used a silicon dioxide (SiO_2) as a grating material, since its refractive index is similar to that of natural *Morpho* wings. Other materials with different refractive index (i.e., silicon nitride (SiN_x), zinc sulfide (ZnS), and gallium phosphide (GaP)) were also used for exploring the influence of material information on the reflectance characteristics. The structures can be fabricated by the previously reported methods [16–21]. The calculations of diffractive power of nanophotonic structures were conducted by using a rigorous coupled-wave analysis (RCWA) method and materials dispersion/absorption was also considered.

Figures 2(a) and 2(b) show the contour map of reflectance variation of simple *Morpho* structures as a function of wavelength (300 nm–800 nm) and thickness of (a) slab and (b) air gap. As expected, the initial structure (white line) shows excellent reflection spectra (>80%) at blue wavelength (~460 nm), while maintaining low reflections at all other wavelengths. Such spectra have similar tendency with that of one-dimensional photonic crystal slabs. The stop band (i.e., the regions for high reflectance) is ~100 nm. Since the basic principle for generating the vivid color is the thin-film multilayer interference, the reflection peak shifts to the shorter wavelength as the slab thickness (t_1) decreases (Figure 2(a)). The thickness of air gap also affects the wavelength shift and the movement ratio is almost the same as the effect of slab thickness (Figure 2(b)). In case of very thin slab thickness ($t_1 < 40$ nm in Figure 2(a)), the optical response (reflected power and stop band) rapidly decreases. It is noted that the effect of thickness variation on the reflection curves is remarkably reduced when the total thickness of single pair (i.e., $t_1 + t_2$) is fixed, as depicted in Figure 2(c). In case of lithography-based nanofabrication, development process after lithography usually determines the thicknesses (t_1 and t_2), while it maintains the total thickness of each pair. In this point of view, it is needed to consider that the thickness variation of 1 nm results in ~1 nm shift of reflection curve, based on Figure 2(c). By contrast, the results shown in Figures 2(a) and 2(b) should be considered in the fabrication based on the multilayer deposition.

The diminishing effect of reflectance can be also found in the structures with a large period, because the space gap between ridges does not affect the reflection. To visualize such effect, we calculated the electric-field distribution of *Morpho* structures, as shown in Figure 3(b). If the period reaches the lamella width (i.e., nearly continuous connection of slab), the structure affords maximum reflectance, while sustaining the low reflectance at other wavelengths (top and middle in Figure 3(b)). On the other hand, the structures with a large period (bottom in Figure 3(b)) provide high reflectance at only limited areas, resulting in degrading the optical response. Usually, the closely packed structures impose a heavy burden on the fabrication procedure. The structures need to have few-tens-of-nanometers gaps between the slabs by considering the lithography margins.

Basically, the *Morpho* structures generate strong light reflections through a combination of multilayer interference of light on their lamella and light-diffraction effect on their array of ridges. Figure 4 shows the reflectance variations of *Morpho* structures with different lamella widths (300, 636, and 1000 nm) and ridge widths (0, 64, and 128 nm). *Morpho* structures without ridges (Figure 4(a)) show the highest reflectance and broaden reflection band compared to that of structures with ridges (Figures 4(b) and 4(c)). With ridges of 64 nm, these structures have slightly narrow stop bands, resulting in improved color purity. On the other hand, increased ridge width has adverse effect on the reflection power, due to strong light diffraction from the ridges. It is also noted that these hierarchical structures generate higher order diffracted reflection when the period is larger than incident wavelength. Hence, reasonable ridge widths should be selected from these calculation results.

In a one-dimensional photonic crystal, the photonic band gap strongly depends on the refractive indices as well as the thicknesses of consisting materials. Figure 5 depicts the effect of refractive index of the structure and surrounding medium on the reflectance spectra variation. The material candidates for *Morpho* structure are mostly found in semiconductor or dielectric materials with refractive index of 1.5 to 3.5. Since

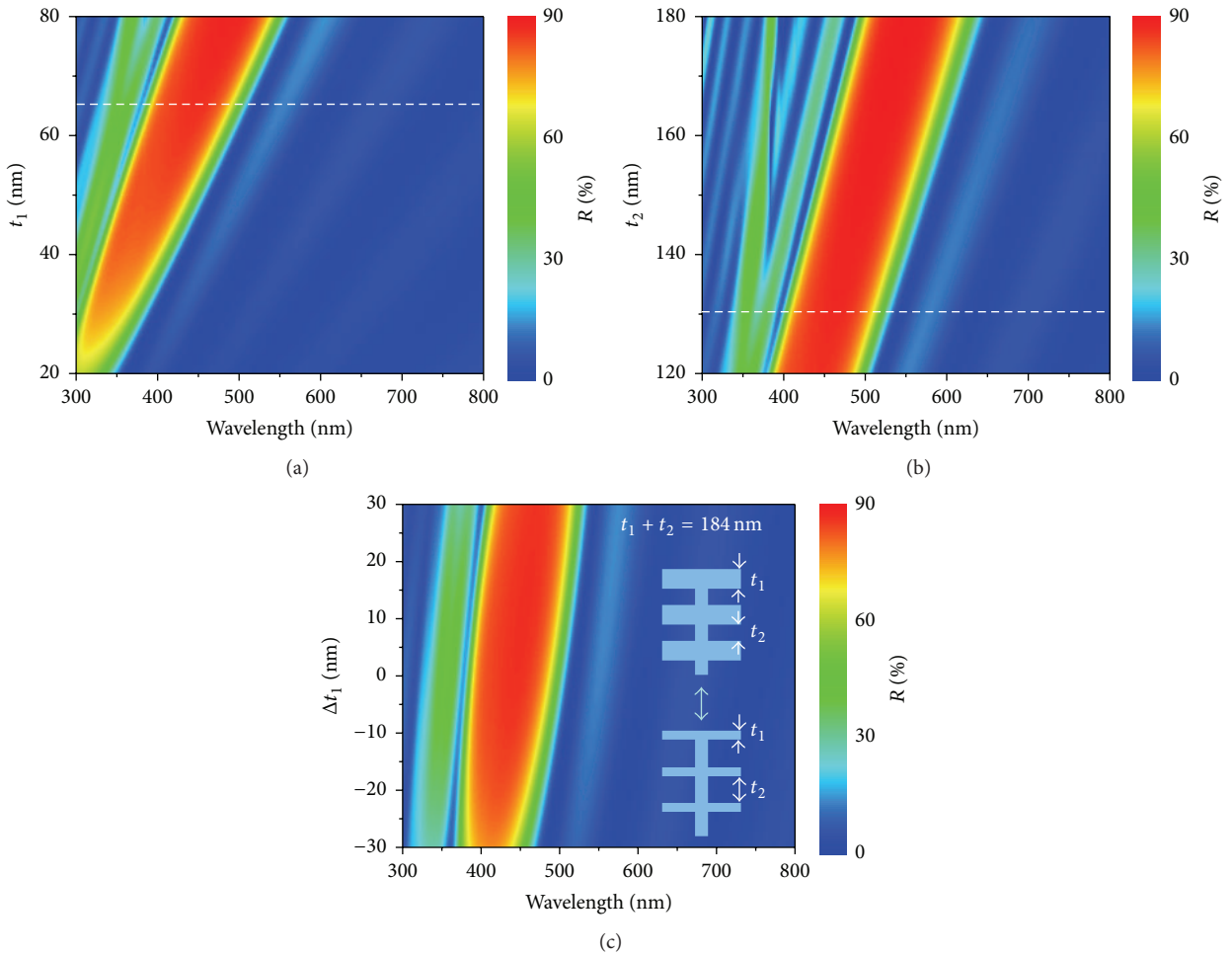

FIGURE 2: Contour plot of the reflectance spectra of photonic-nanostructures as a function of (a) slab thickness (t_1), (b) air gap thickness (t_2), and (c) slab thickness variation (Δt_1) with fixed total thickness (i.e., $t_1 + t_2$). White dashed lines in (a) and (b) indicate the initial thickness obtained from natural *Morpho* butterfly.

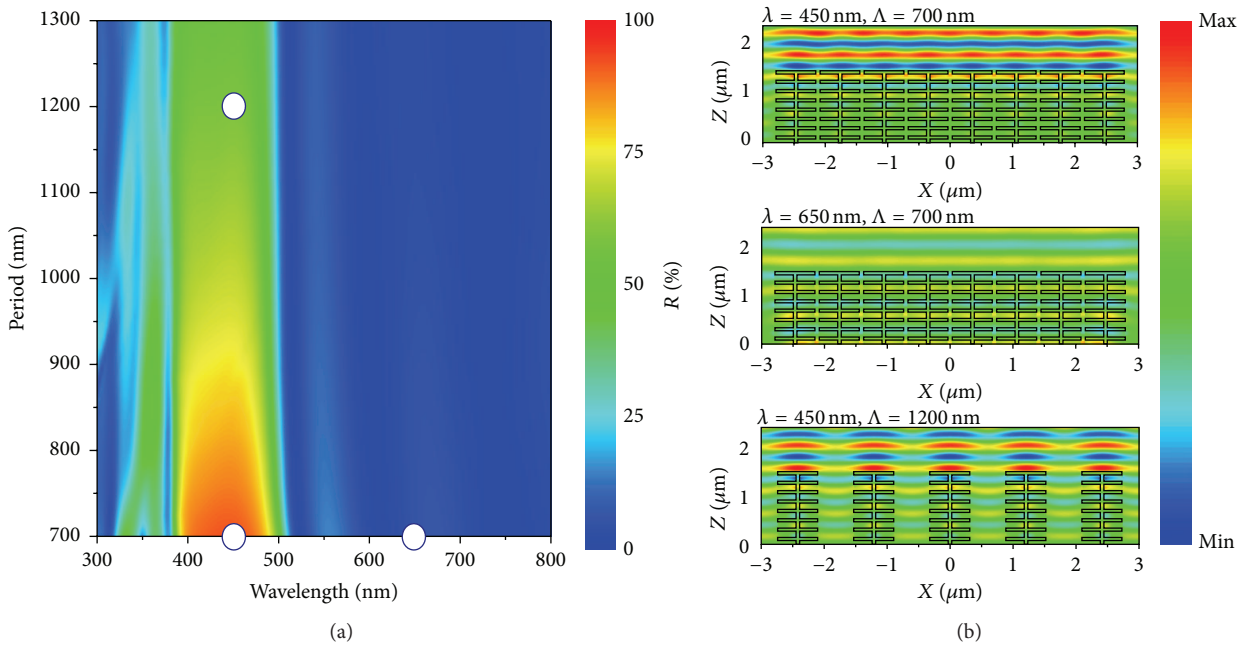

FIGURE 3: (a) Contour plot of the reflectance of *Morpho* nanostructure as a function of wavelength and period, (b) E-field profiles of *Morpho* nanostructures for three different positions indicated in (a).

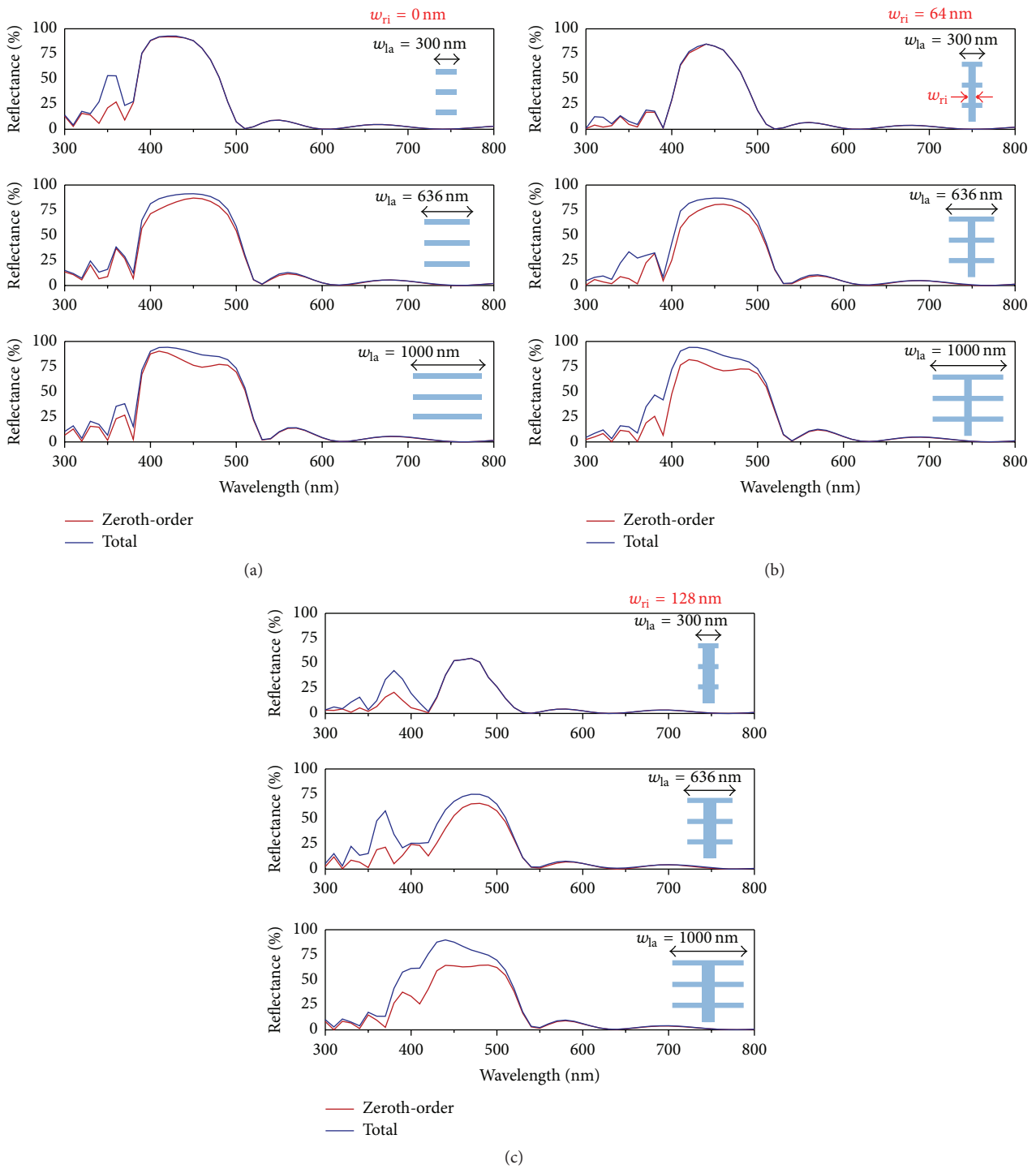

FIGURE 4: Total reflectance of *Morpho* structures for three different ridge widths (w_{ri}), that is, (a) 0 nm, (b) 64 nm, and (c) 128 nm, respectively, with three different lamella widths (300 nm, 636 nm, and 1000 nm). As a reference, zeroth-order reflectance is inserted in each figure.

the peak reflectance relates to the optical thickness of low and high index materials (i.e., $\lambda/4n_L$ and $\lambda/4n_H$), higher structure index provides redshifted peak wavelength. In this geometry, the structure index should be less than 2.5 for the use of this structure in the visible ranges. As the structure index increases, the stop band enlarges due to the enhanced index gap between low and high index materials. It is noted that this broaden optical band does not present single color but mixed one, which is not suitable for optical sensing. In case of gas, vapor, or liquid sensing applications, the refractive index of

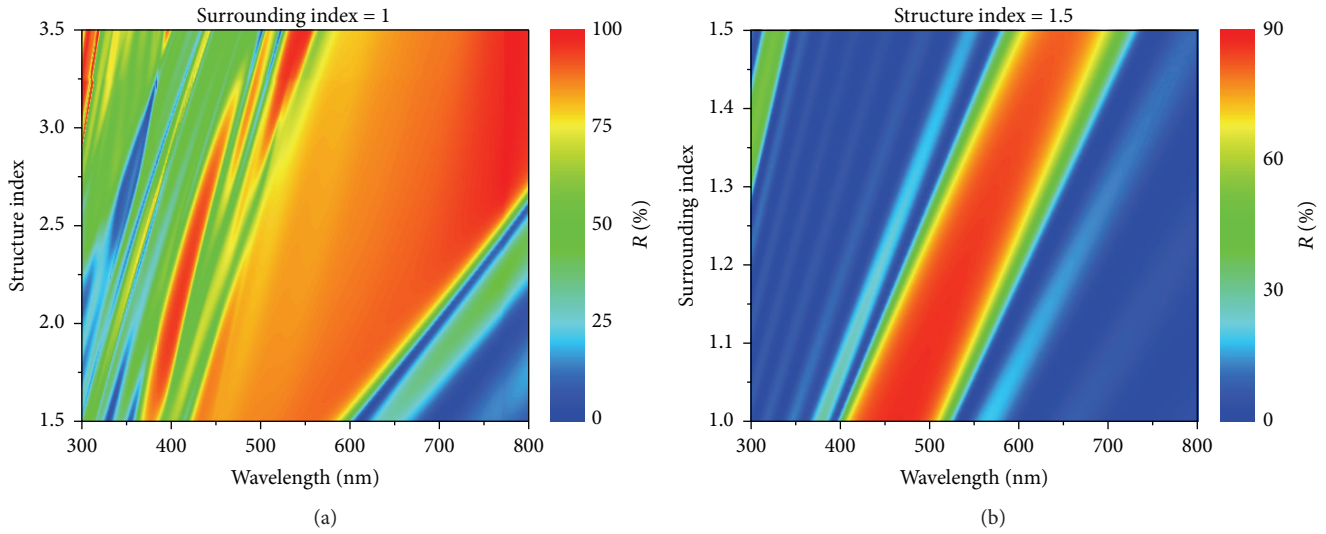

FIGURE 5: Contour map of the reflectance variation of photonic-nanostructures (a) with various structure indices and (b) various surrounding indices.

surrounding medium would be changed from 1.0 to 1.3. As can be seen in Figure 5(b), remarkable redshift occurs during the surrounding index changes. The peak wavelength of the structure with a refractive index of 1.5 changes from 460 nm to 580 nm, as the surrounding index increases from 1.0 to 1.3. These characteristics would be ideal for highly sensitive gas sensors.

Figure 6 provides more detailed spectra for practical sensing applications. In this calculation, we selected four different materials (i.e., SiO_2, SiN_x, ZnS, and GaP), which are frequently used in the semiconductor industry and compatible to the complementary metal oxide semiconductor fabrication technology. For dielectric materials, the fabrication process would contain conventional deposition process by using a sputtering or e-beam evaporation followed by selective etching of low index materials to define the air gap. In case of semiconductor materials, the epitaxial growth of each layer can be conducted via molecular beam epitaxy (MBE) and refractive indices of these four materials that are in the range of 1.55 (SiO_2) to 3.3 (GaP). For the use of these materials in the visible ranges, the geometry of the structures except for SiO_2 was slightly modified. In all cases, the reflectance spectra move to longer wavelength region with similar steps (0.7~0.9 nm per 0.02 index variation (Δn)), as the surround index increases from 1.0 to 1.1. However, this similar tendency does not provide homogeneous color sensitivity due to the large difference of stop band width and shape of reflectance curves. As indicated in Figure 6(b), higher index materials have high reflection in broad wavelength ranges.

One of the easiest ways to visualize the color sensitivity/variation is the use of CIE chromaticity diagram. Figure 6(c) shows the CIE plots for the reflectance changes of *Morpho* structures with four different materials and varying surround index. We used 1931 CIE color matching functions to indicate each reflectance spectrum on the CIE chromaticity diagram. As illustrated in Figure 6(b), the structure with SiO_2 has strong color difference from blue to bluish green. The SiN_x also have abrupt changes in CIE diagram; however, the colors are distributed near the center region. This means that the colors are not distinguishable from that of SiO_2 because of their low saturation level. In this point of view, low index materials are more appropriate for optical sensing applications. On the other hand, high index materials have colors near white regions and the position differences are not abrupt. Hence, these materials are not applicable for high sensitive optical systems. Instead, this optical performance would be applicable to broadband optical reflectors without metallic materials or dyes.

3. Conclusions

By considering the fabrication procedure and material issues, we investigated optimum geometry of artificial *Morpho* nanostructures for optical sensing applications. From the contour plots, the effects of the widths, periods, thicknesses, and refractive indices on the reflectance were also analyzed. The *Morpho* nanostructures with optimized geometry can be used for various applications including gas or vapor sensors, health monitoring color indicator, immersion type liquid checker, and photonic circuits. Extension to flexible forms of such color indicator would be one of the future directions for wearable electronics.

Conflict of Interests

The authors declare that there is no conflict of interests regarding the publication of this paper.

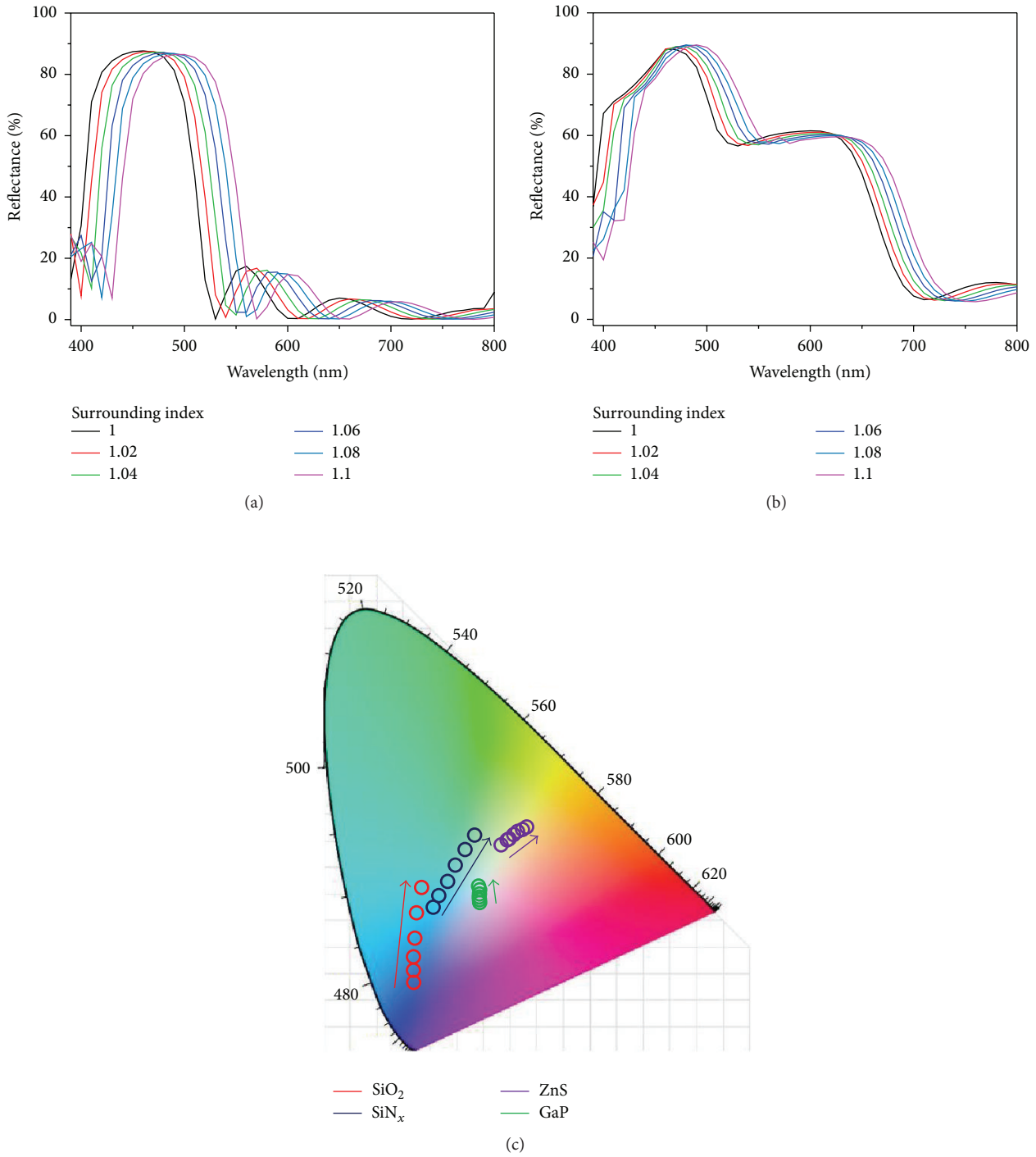

FIGURE 6: Reflectance curves of *Morpho* structures for two different materials ((a) SiO_2 and (b) GaP) with varying surrounding indices (from 1.0 to 1.1 with 0.02 steps), (c) CIE plots of reflectance spectra for *Morpho* structures with four different materials (i.e., SiO_2, SiN_x, ZnS, and GaP). Arrows indicate directions for surround index increment.

Acknowledgments

This work was supported by the National Research Foundation of Korea (NRF) Grant funded by the Korean Government (MSIP) (no. 2015R1A5A7036513).

References

[1] S. Kinoshita, S. Yoshioka, and J. Miyazaki, "Physics of structural colors," *Reports on Progress in Physics*, vol. 71, no. 7, Article ID 076401, 2008.

[2] S. Berthier, E. Charron, and J. Boulenguez, "Morphological structure and optical properties of the wings of Morphidae," *Insect Science*, vol. 13, no. 2, pp. 145–158, 2006.

[3] S. Kinoshita and S. Yoshioka, "Structural colors in nature: the role of regularity and irregularity in the structure," *ChemPhysChem*, vol. 6, no. 8, pp. 1443–1459, 2005.

[4] S. Yoshioka and S. Kinoshita, "Structural or pigmentary? Origin of the distinctive white stripe on the blue wing of a Morpho butterfly," *Proceedings of the Royal Society B: Biological Sciences*, vol. 273, no. 1583, pp. 129–134, 2006.

[5] G. Tayeb, B. Gralak, and S. Enoch, "Structural colors in nature and butterfly-wing modeling," *Optics and Photonics News*, vol. 14, no. 2, pp. 38–49, 2003.

[6] Y. Ding, S. Xu, and Z. L. Wang, "Structural colors from Morpho peleides butterfly wing scales," *Journal of Applied Physics*, vol. 106, no. 7, Article ID 074702, 2009.

[7] B. R. Wasik, S. F. Liew, D. A. Lilien et al., "Artificial selection for structural color on butterfly wings and comparison with natural evolution," *Proceedings of the National Academy of Sciences of the United States of America*, vol. 111, no. 33, pp. 12109–12114, 2014.

[8] R. T. Lee and G. S. Smith, "Detailed electromagnetic simulation for the structural color of butterfly wings," *Applied Optics*, vol. 48, no. 21, pp. 4177–4190, 2009.

[9] L. Plattner, "Optical properties of the scales of *Morpho rhetenor* butterflies: theoretical and experimental investigation of the back-scattering of light in the visible spectrum," *Journal of the Royal Society Interface*, vol. 1, no. 1, pp. 49–59, 2004.

[10] B. Gralak, G. Tayeb, and S. Enoch, "Morpho butterflies wings color modeled with lamellar grating theory," *Optics Express*, vol. 9, no. 11, pp. 567–578, 2001.

[11] R. H. Siddique, S. Diewald, J. Leuthold, and H. Hölscher, "Theoretical and experimental analysis of the structural pattern responsible for the iridescence of *Morpho* butterflies," *Optics Express*, vol. 21, no. 12, pp. 14351–14361, 2013.

[12] K. Watanabe, T. Hoshino, K. Kanda, Y. Haruyama, and S. Matsui, "Brilliant blue observation from a morpho-butterfly-scale quasi-structure," *Japanese Journal of Applied Physics, Part 2: Letters*, vol. 44, part 2, no. 1–7, p. L48, 2005.

[13] R. A. Potyrailo, H. Ghiradella, A. Vertiatchikh, K. Dovidenko, J. R. Cournoyer, and E. Olson, "*Morpho* butterfly wing scales demonstrate highly selective vapour response," *Nature Photonics*, vol. 1, no. 2, pp. 123–128, 2007.

[14] Z. Han, S. Niu, M. Yang et al., "Unparalleled sensitivity of photonic structures in butterfly wings," *RSC Advances*, vol. 4, no. 85, pp. 45214–45219, 2014.

[15] L. P. Biro, K. Kertesz, Z. Vertesy, and Z. Balint, "Photonic nanoarchitectures occurring in butterfly scales as selective gas/vapor sensors," in *The Nature of Light: Light in Nature II*, vol. 7057 of *Proceedings of SPIE*, Katherine Creath, San Diego, Calif, USA, August 2008.

[16] W. Wu, G. Liao, T. Shi, R. Malik, and C. Zeng, "The relationship of selective surrounding response and the nanophotonic structures of *Morpho* butterfly scales," *Microelectronic Engineering*, vol. 95, pp. 42–48, 2012.

[17] H. Wang and K.-Q. Zhang, "Photonic crystal structures with tunable structure color as colorimetric sensors," *Sensors*, vol. 13, no. 4, pp. 4192–4213, 2013.

[18] C. Fenzl, T. Hirsch, and O. S. Wolfbeis, "Photonic crystals for chemical sensing and biosensing," *Angewandte Chemie—International Edition*, vol. 53, no. 13, pp. 3318–3335, 2014.

[19] R. H. Siddique, R. Hünig, A. Faisal, U. Lemmer, and H. Hölscher, "Fabrication of hierarchical photonic nanostructures inspired by *Morpho* butterflies utilizing laser interference lithography," *Optical Materials Express*, vol. 5, no. 5, pp. 996–1005, 2015.

[20] M. Aryal, D.-H. Ko, J. R. Tumbleston, A. Gadisa, E. T. Samulski, and R. Lopez, "Large area nanofabrication of butterfly wings three dimensional ultrastructures," *Journal of Vacuum Science and Technology B: Nanotechnology and Microelectronics*, vol. 30, no. 6, Article ID 061802, 2012.

[21] R. A. Potyrailo, R. K. Bonam, J. G. Hartley et al., "Towards outperforming conventional sensor arrays with fabricated individual photonic vapour sensors inspired by *Morpho* butterflies," *Nature Communications*, vol. 6, article 7959, 2015.

[22] H. Xu, P. Wu, C. Zhu, A. Elbaz, and Z. Z. Gu, "Photonic crystal for gas sensing," *Journal of Materials Chemistry C*, vol. 1, no. 38, pp. 6087–6098, 2013.

[23] S. Zhu, D. Zhang, Z. Chen et al., "A simple and effective approach towards biomimetic replication of photonic structures from butterfly wings," *Nanotechnology*, vol. 20, no. 31, Article ID 315303, 2009.